AD-A060 900 NAVAL RESEARCH LAB WASHINGTON D C F/G 8/7

ROTATIONAL DEFORMATION OF THE EARTH AND MAJOR PLANETS.(U)

AUG 78 P LANZANO, J C DALEY

UNCLASSIFIED NRL-8252 NL

1 OF 1

AD A060900

END

DATE FILMED

1-79

DDC

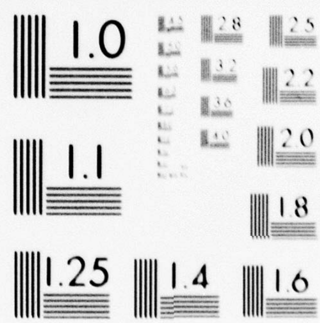

MICROCOPY RESOLUTION TEST CHART

NRL Report 8252

Rotational Deformation of the Earth and Major Planets

Paolo Lanzano and John C. Daley
Space Systems Division

August 18, 1978

NAVAL RESEARCH LABORATORY
Washington, D.C.

SECURITY CLASSIFICATION OF THIS PAGE (When Data Entered)

REPORT DOCUMENTATION PAGE		READ INSTRUCTIONS BEFORE COMPLETING FORM
1. REPORT NUMBER NRL Report 8252	2. GOVT ACCESSION NO.	3. RECIPIENT'S CATALOG NUMBER
4. TITLE (and Subtitle) ROTATIONAL DEFORMATION OF THE EARTH AND MAJOR PLANETS		5. TYPE OF REPORT & PERIOD COVERED A final report on one phase of a continuing NRL problem
		6. PERFORMING ORG. REPORT NUMBER
7. AUTHOR(s) Paolo Lanzano and John C. Daley		8. CONTRACT OR GRANT NUMBER(s)
9. PERFORMING ORGANIZATION NAME AND ADDRESS Naval Research Laboratory Washington, D.C. 20375 251 950		10. PROGRAM ELEMENT, PROJECT, TASK AREA & WORK UNIT NUMBERS B01-22
11. CONTROLLING OFFICE NAME AND ADDRESS Department of the Navy Office of Naval Research Arlington, Virginia 22217		12. REPORT DATE August 18, 1978
		13. NUMBER OF PAGES 27
14. MONITORING AGENCY NAME & ADDRESS (if different from Controlling Office) (14) NRL-8252		15. SECURITY CLASS. (of this report) Unclassified
		15a. DECLASSIFICATION/DOWNGRADING SCHEDULE

16. DISTRIBUTION STATEMENT (of this Report)

Approved for public release; distribution unlimited

(11) 18 Aug 78 (12) 28p.

17. DISTRIBUTION STATEMENT (of the abstract entered in Block 20, if different from Report)

(9) Final rept.

DDC RECEIVED NOV 6 1978 B

18. SUPPLEMENTARY NOTES

19. KEY WORDS (Continue on reverse side if necessary and identify by block number)

Clairaut equation
Navier-Stokes equation
Earth density model
Deformation coefficients
Geoid
Planetary elasticity
Planetary interiors
Jupiter's and Saturn's oblateness

20. ABSTRACT (Continue on reverse side if necessary and identify by block number)

~~We apply our~~ recently developed third-order theory of hydrostatic equilibrium to study the deformations which the Earth, Jupiter, and Saturn undergo because of their rotational motion were applied.
For the Earth, ~~we~~ input the Bullen, HB1, 1066A, and QM2 density models to solve the Clairaut equation numerically and compare ~~our~~ the results with data obtained from satellites. A linearized version of the Navier-Stokes equation is next developed to take into account the elastic characteristics of the Earth and to model the shear stresses and convection currents existing in the Earth's upper layers. The numerical solution of this last equation, however, is left for future reporting.

DD FORM 1 JAN 73 1473 EDITION OF 1 NOV 65 IS OBSOLETE
S/N 0102-014-6601

i SECURITY CLASSIFICATION OF THIS PAGE (When Data Entered)

78 10 23 056 251 950

20. ABSTRACT (Continued):

For Jupiter and Saturn we use the DeMarcus density profile in conjunction with the Brouwer and Clemence data and compare our results with an older attempt and some recent work based on a different density profile and a less sophisticated equilibrium theory. Our third-order theory leads to the Clairaut equation with boundary conditions and is amenable to a rapid and accurate numerical solution. Our method appears to be an improvement to the present state of the art in planetology; we avoid the use of complicated systems of integral equations that are difficult to solve numerically.

CONTENTS

ROTATIONAL DEFORMATION OF THE EARTH AND MAJOR PLANETS

INTRODUCTION

The purpose of this paper is to ascertain the deformations sustained by a rotating self-gravitating massive body when hydrostatic and elastic forces are present within its interior. There are many advantages to be gained by studies of this type of deformation; for example: (1) better determination of the shape of the geoid in conjunction with accurate gravity measurements, (2) better knowledge of the Earth's bodily tides and of the Love numbers, (3) effects of crustal loading on the global ocean tides, and (4) determination of the gravity field of a planet.

The Earth and/or any other planet are considered to be initially in hydrostatic equilibrium under the influence of self-gravitatation and of their rotational motion. This initial state of deformation will be taken as the reference state.

The following relationships will be valid between the stress field T_{ij} and the hydrostatic pressure p_0:

$$T_{ij} = -p_0 \delta_{ij}; \quad \frac{\partial p_0}{\partial x_i} = \rho_0 g_{0,i} \ . \tag{1}$$

Here the δ's are the Kronecker deltas, and ρ_0 is the mass density of the reference state. $g_{0,i}$ are the components of gravity for the same state and are obtainable from the gravity potential as

$$g_{0,i} = \frac{\partial V_0}{\partial x_i} \ . \tag{2}$$

This potential is the sum of two terms: the gravitational potential V_0^* and the rotational potential

$$V_c = \frac{1}{2} \ \omega^2 r^2 \sin^2\theta, \tag{3}$$

where ω is the rotational velocity, r is the radius vector measured from the center of gravity, and θ is the colatitude. V_0 satisfies the Poisson equation

$$\nabla^2 V_0 = -4\pi G \rho_0 + 2\omega^2, \tag{4}$$

where G is the gravitational constant.

Manuscript submitted June 9, 1978.

In previous publications — Lanzano [1] and Kopal and Lanzano [2] — we used equation (1) to ascertain how within a massive rotating configuration the equipotential surfaces which were originally of spherical shape are deformed into spheroids having an equation of the sort

$$\frac{r}{a} = 1 + \sum_{j=0}^{\infty} f_{2j} \left(\frac{a}{a_1}\right) P_{2j} (\cos \theta). \tag{5}$$

Here the parameter a denotes the mean radius of the spheroid, a_1 corresponds to the outermost equipotential surface, and the P's are, as usual, the Legendre polynomials. The deformation coefficients were in turn expressed as power series of the dimensionless parameter

$$q = \frac{\omega^2 a_1^3}{3Gm_1}, \tag{6}$$

where m_1 is the mass of the total configuration. This parameter essentially represents the ratio between centrifugal and gravitational accelerations. The accepted value of q for the Earth is 0.00115, for Jupiter 0.028004, and for Saturn 0.047207. In the aforementioned publications, we developed an equilibrium theory valid up to the third power of q; we limited ourselves to the following expansions:

$$\begin{aligned} f_0 &= \phantom{qf_{21}} \quad\; q^2 f_{02} + q^3 f_{03} \\ f_2 &= q f_{21} + q^2 f_{22} + q^3 f_{23} \\ f_4 &= \phantom{qf_{21}} \quad\; q^2 f_{42} + q^3 f_{43} \\ f_6 &= \phantom{qf_{21} + q^2 f_{22}} \quad\;\; q^3 f_{63}\,. \end{aligned} \tag{7}$$

The unknown functions f_{02} and f_{03} were eliminated via mass conservation considerations and found to be related to f_{21} and f_{22} as follows:

$$f_{02} = -\frac{1}{5} f_{21}^2; \quad f_{03} = -\frac{2}{5} f_{21} \left(f_{22} + \frac{1}{21} f_{21}^2\right). \tag{8}$$

The other six unknown deformation coefficients (i.e., $f_{21}, f_{22}, f_{23}; f_{42}, f_{43}; f_{63}$) were found to satisfy a boundary value differential system consisting of the Clairaut equations

$$a^2 f'' + 6aDf' + (6D - C) f = R \tag{9}$$

with the following conditions at both ends of the interval $(0, a_1)$:

$$f(0) = f'(0) = 0$$

$$A f(a_1) + B f'(a_1) = S(a_1). \tag{10}$$

Here the primes denote derivatives with respect to the mean radius a, and A, B, C are constants depending on the order of approximation. The function

$$D(a) = \rho_0(a)/\bar{\rho}_0(a) \tag{11}$$

is the ratio between the density $\rho_0(a)$ and the mean density

$$\bar{\rho}_0(a) = \frac{3}{a^3}\int_0^a \rho_0 a^2 da. \tag{12}$$

$R(a)$ and $S(a)$ are known functions of a that depend on lower order approximations.

The specific values of the constants and the form of the functions appearing in equations (9) and (10) were given in the above mentioned papers and will not be reproduced here.

EARTH DENSITY MODELS

One must integrate the Clairaut equation to obtain the ellipticity of the equipotential surfaces as well as the rotational deformation of the outermost equilibrium surface. For this purpose, a density profile $\rho_0(r)$ should be provided. In this paper we plan to take into consideration recent Earth density models, to integrate the Clairaut equation, and to compare results pertaining to the exterior potential with data obtainable from satellite geodesy.

In a recent paper, Lanzano and Daley [3], the Haddon and Bullen 1969 HB1 Earth density model was discussed and the results of the numerical integration were compared with earlier work by James and Kopal [4]. For numerical integration purposes we have used here the 1975 1066A Earth density model by Gilbert and Dziewonski and the 1977 QM2 model by Anderson and Hart.

A brief discussion of these models appears appropriate and will be provided here to enable the reader to understand their relative merits and limitations and thereby comprehend the validity of the numerical results.

Bullen has provided the first approximate Earth models by pioneering work in which he used the fact that the travel times of the bodily waves do not depend upon the source mechanism of the earthquake but are functionals of structure alone. These models were achieved by relating the travel time with the travelled angular distance and by making use of the following equations:

$$\alpha^2 = \frac{k}{\rho_0} + \frac{4}{3}\beta^2; \quad \beta^2 = \frac{\mu}{\rho_0}; \quad \frac{d\rho_0}{dz} = \eta\rho_0^2 g_0/k, \tag{13}$$

where k, μ, α, β denote, respectively, the incompressibility, the rigidity, and the P and S seismic velocities at depth z from the surface or at distance r from the center; here η is a coefficient depending on the homogeneity of the material (see, e.g., Bullen [5], pp. 227-240).

These early Bullen models were used by Kopal [4] to determine the second and fourth harmonics of the geopotential from hydrostatic theory alone by integrating a second-order approximation of the Clairaut equation.

Improvements to these early models, which were based on travel time data alone, can be obtained by making use of the observed frequencies of the Earth vibrations caused by earthquakes. These vibrations can be construed as being the superposition of the elastic-gravitational normal modes of the Earth that are excited by an earthquake. One can construct average Earth models through the inversion of the observed eigenperiods of the Earth. Mathematically the problem consists of finding perturbations to a given Earth model so that the differences between calculated and observed eigenfrequencies can be minimized.

The normal modes of oscillation for a nonrotating, spherically symmetric Earth are of two kinds: spheroidal and toroidal. The amplitudes of their oscillations are representable, respectively, as

$$
\begin{aligned}
{}_nS_\ell^m &= {}_nU_\ell(r)Y_\ell^m(\theta,\phi)\,\mathbf{r} + {}_nV_\ell(r)r\nabla Y_\ell^m(\theta,\phi),\\
{}_nT_\ell^m &= -{}_nW_\ell(r)\,\mathbf{r}\times\nabla Y_\ell^m(\theta,\phi).
\end{aligned}
\tag{14}
$$

These oscillations depend on three parameters: the angular order ℓ, the azimuthal order m (with $-\ell \leq m \leq \ell$) — which are related to the degree ℓ and order m of the spherical harmonic $Y_\ell^m(\theta,\phi)$ — and the radial number n, which defines the overtone.

The azimuthal order m does not appear in the differential equations or boundary conditions, so that for each ℓ and n there are $2\ell + 1$ normal mode eigenfunctions, all of which belong to the same eigenfrequency; together they form a multiplet. This phenomenon is called degeneracy and constitutes the main difficulty in identifying spectral peaks of the eigenfrequencies and in comparing them with theoretical calculations. Perturbations, such as rotation, ellipticity, and geographical features remove the degeneracy of a multiplet and lead to a split multiplet. Ascertaining the splitting parameters of a multiplet would be a step leading to the possibility of solving for singlets; however, the theory behind such splitting is not well understood and consequently has not been formulated. Accordingly, all the Earth models available up to the present time are based on a nonrotating Earth. On the other hand, new developments in instrumentation allow geophysicists to lower the detection threshold for magnitudes in the low frequency modes and thus increase the number of usable seismic events.

In the 1969 HB1 Earth model by Haddon and Bullen [6], 110 observations of periods of spheroidal and toroidal oscillations were taken into account based on the earthquakes of May 1960 in Chile and March 1964 in Alaska. Also, for the first time, use was made of: (1) the revised value of the Earth's polar moment of inertia: $I_p = 0.3309\ m_1 a_1^2$, where $m_1 = 5.976.10^{27}$g is the Earth's total mass and $a_1 = 6371$ km is the Earth's mean radius (i.e., the radius of a sphere of equal volume) and (2) the evidence that the central density ρ_c is ≤ 13 g/cm^3.

In the preceding as well as in many other free oscillation studies of the Earth's interior, the effect of absorption upon the eigenperiods of the Earth has been ignored: this is equivalent to assuming that the Earth is perfectly elastic. The actual Earth is significantly anelestic over seismic frequencies, and recent research by Hart et al. [7] has revealed that a frequency-dependent correction of the order of 1% should be applied to the normal mode periods to eliminate baseline discrepancies between body wave results and normal mode results. These authors adjusted the eigenperiods of their older C2 Earth model for attenuation and then by inversion obtained the QM2 model (1977). Inclusion of the attenuation term tends to increase the values of seismic velocities, especially the shear velocity.

All the methods mentioned are based on dispersion characteristics of traveling waves, the eigenfrequencies of normal modes, and the attenuations of both, which are essentially functionals of the Earth structure alone. A complementary procedure for improving upon the mechanical model of the Earth is to study the source mechanism of an earthquake from the knowledge of the normal mode amplitudes. Using both methods one can then initiate an iterative process of successive refinements of structure and mechanism.

This is essentially the procedure followed by Gilbert and Dziewonski [8] in obtaining their 1066A model in 1975. The gross Earth data were compiled from 1461 modes, whereas the source mechanism (or moment tensor) was retrieved from the seismic spectra of the July 1970 Colombia and the August 1963 Peru-Bolivia earthquakes. Tables 1, 2, and 3 represent the density variations with depth for the HB1, 1066A and QM2 models, respectively.

NUMERICAL INTEGRATION OF THE CLAIRAUT EQUATIONS AND RESULTING EARTH DEFORMATIONS

We have used central difference formulas to express the first and second derivatives of the unknown functions at the various pivotal points chosen within the integration range. Neglecting third and higher order central difference terms and assuming equal intervals between the pivotal points, we find that the Clairaut equation (9) takes the form of a three-term set of difference equations:

$$A(i,1)f_{i-1} + A(i,2)f_i + A(i,3)f_{i+1} = A(i,4); (i = 1,2, \ldots, N), \tag{15}$$

where the subscript i refers to the pivotal point at which the functions are evaluated, and the A's depend on the coefficients of the original equation and the interval size.

Table 1 — Values of Density ρ, in the Earth Model HB1

Depth (km)	ρ (g/cm^3)	Depth	ρ	Depth	ρ
0	2.840	984	4.529	3600	10.948
15	2.840	1000	4.538	3800	11.176
15	3.313	1200	4.655	4000	11.383
60	3.332	1400	4.768	4200	11.570
100	3.348	1600	4.877	4400	11.737
200	3.387	1800	4.983	4600	11.887
300	3.424	2000	5.087	4800	12.017
350	3.441	2200	5.188	4982	12.121
350	3.700	2400	5.288	5000	12.130
400	3.775	2600	5.387	5121	12.197
413	3.795	2800	5.487	5200	12.229
500	3.925	2878	5.527	5400	12.301
600	4.075	2878	9.927	5600	12.360
650	4.150	3000	10.121	5800	12.405
650	4.200	3200	10.421	6000	12.437
800	4.380	3400	10.697	6200	12.455
				6371	12.460

Table 2 — Values of Density ρ, in the Earth Model 1066A

Depth (km)	ρ (g/cm^3)	Depth	ρ	Depth	ρ	Depth	ρ
0	2.183	1,121	4.635	2,576	5.421	5,142	12.153
6	2.183	1,156	4.660	2,610	5.434	5,142	13.021
11	2.183	1,191	4.683	2,645	5.447	5,181	13.031
11	3.343	1,225	4.705	2,680	5.460	5,219	13.045
37	3.351	1,260	4.724	2,714	5.471	5,257	13.060
62	3.358	1,294	4.741	2,749	5.483	5,296	13.074
88	3.365	1,329	4.756	2,784	5.495	5,334	13.088
114	3.372	1,364	4.770	2,818	5.506	5,373	13.102
139	3.379	1,398	4.783	2,853	5.518	5,411	13.116
165	3.387	1,433	4.797	2,887	5.528	5,449	13.131
190	3.393	1,468	4.811	2,887	9.914	5.488	13.145
216	3.402	1,502	4.825	2,958	10.028	5,526	13.160
242	3.419	1,537	4.841	3,028	10.134	5,565	13.175
267	3.443	1,571	4.857	3,099	10.235	5,603	13.190
293	3.473	1,606	4.874	3,169	10.333	5,641	13.205
319	3.509	1,641	4.892	3,240	10.427	5,680	13.220
344	3.551	1,675	4.911	3,310	10.516	5,718	13.235
370	3.600	1,710	4.930	3,381	10.603	5,757	13.251
395	3.657	1,745	4.949	3,451	10.687	5,795	13.267
421	3.712	1,779	4.969	3,522	10.772	5,833	13.284
421	3.712	1,814	4.988	3,592	10.858	5,872	13.300
452	3.764	1,849	5.008	3,663	10.946	5,910	13.316
484	3.805	1,883	5.027	3,733	11.033	5,949	13.331
515	3.850	1,918	5.046	3,803	11.116	5,987	13.345
546	3.903	1,952	5.066	3,874	11.192	6,025	13.357
577	3.961	1,987	5.086	3,944	11.265	6,064	13.368
609	4.025	2,022	5.106	4,015	11.335	6,102	13.377
640	4.106	2,056	5.127	4,085	11.406	6,141	13.385
671	4.208	2,091	5.147	4,156	11.475	6,179	13.393
671	4.208	2,126	5.169	4,226	11.541	6,217	13.399
706	4.319	2,160	5.190	4,297	11.602	6,256	13.406
740	4.403	2,195	5.212	4,367	11.660	6,294	13.411
775	4.468	2,229	5.233	4,438	11.716	6,333	13.418
810	4.511	2,264	5.255	4,508	11.769	6,371	13.421
844	4.535	2,299	5.277	4,578	11.818		
879	4.537	2,333	5.298	4,649	11.863		
913	4.537	2,368	5.318	4,719	11.904		
948	4.542	2,403	5.338	4,790	11.944		
983	4.552	2,437	5.357	4,860	11.985		
1,017	4.567	2,472	5.374	4,931	12.026		
1,052	4.587	2,507	5.391	5,001	12.068		
1,087	4.610	2,541	5.406	5,072	12.110		

Table 3 — Values of Density ρ, in the Earth Model QM2

Depth (km)	ρ (g/cm^3)	Depth	ρ	Depth	ρ	Depth	ρ
0	1.02	496	3.72	1546	4.85	3471	10.78
3	1.02	521	3.73	1621	4.89	3571	10.91
3	2.80	546	3.89	1696	4.94	3671	11.02
21	2.80	571	3.95	1771	4.97	3771	11.12
21	3.49	596	3.97	1846	5.01	3871	11.21
41	3.50	621	3.99	1921	5.05	3971	11.29
61	3.52	646	4.00	1996	5.09	4071	11.37
81	3.45	671	4.04	2071	5.14	4171	11.45
101	3.39	671	4.38	2146	5.19	4271	11.53
121	3.31	696	4.40	2221	5.24	4471	11.69
146	3.29	711	4.42	2296	5.29	4571	11.78
171	3.31	728	4.43	2371	5.34	4671	11.85
196	3.33	746	4.44	2446	5.38	4771	11.93
221	3.35	769	4.47	2521	5.42	4871	11.99
246	3.36	798	4.51	2596	5.45	4971	12.05
271	3.36	821	4.52	2671	5.48	5071	12.09
296	3.38	871	4.55	2746	5.49	5156	12.12
321	3.43	946	4.58	2821	5.51	5156	12.30
346	3.51	1021	4.61	2861	5.52	5371	12.48
371	3.59	1096	4.64	2886	5.52	5571	12.52
388	3.63	1171	4.68	2886	9.97	5771	12.52
404	3.71	1246	4.71	2971	10.10	5971	12.52
421	3.82	1321	4.74	3071	10.24	6071	12.53
446	3.81	1396	4.77	3171	10.38	6271	12.57
471	3.76	1471	4.81	3371	10.65	6371	12.57

For this scheme, the values of the f's at two points exterior to the interval of integration must be known; however, this inconvenience can be circumvented by using the two boundary conditions expressed by equation (10).

Due to the discontinuity exhibited by the density profile at the interface of two consecutive layers, one must follow piecewise integration to obtain the mean density $\overline{\rho}_0$ and the related function D. To obtain a unique solution to our integration problem notwithstanding the discontinuous nature of the input data, we have imposed the conditions of continuity for the solutions f and their derivatives f' and have generated the appropriate difference equations according to a procedure developed by Fox [9].

The computations were programmed in Fortran and executed on the Texas Instrument ASC-7 Computer at the Naval Research Laboratory in double precision floating point arithmetic to a precision of 16 decimal digits. An iteration method was employed producing results convergent to at least the 5 decimal digits given in the tables. More details about the integration procedure can be obtained in Lanzano and Daley [3].

Tables 4, 5, and 6 refer to the HB1, 1066A, and QM2 Earth density models, respectively; they furnish the deformation coefficients f_0, f_2, f_4 and f_6 for the equipotential surfaces corresponding to intermediate values of the mean radius a. The number N of pivotal points required to reach the mentioned accuracy was 851, 580, and 607, respectively. The results tabulated at the chosen values of the depth are linear interpolations between the pivotal points.

Table 4 — Deformation Coefficients for the Equipotential Surfaces, Earth Model HB1

Depth (km)	$-10^6 \cdot f_0$	$-10^2 \cdot f_2$	$+10^5 \cdot f_4$	$-10^8 \cdot f_6$
0	0.99421	0.22298	0.44766	0.96569
15	0.99147	0.22268	0.44630	0.96106
300	0.94109	0.21695	0.42139	0.87871
350	0.93259	0.21596	0.41724	0.86551
650	0.88288	0.21013	0.39312	0.79141
900	0.84214	0.20522	0.37324	0.73257
1200	0.79332	0.19918	0.34890	0.66167
1500	0.74495	0.19302	0.32400	0.58968
1800	0.69804	0.18684	0.29891	0.51695
2100	0.65431	0.18089	0.27448	0.44533
2400	0.61654	0.17559	0.25242	0.37940
2878	0.58072	0.17041	0.23085	0.31418
3000	0.57747	0.16994	0.22905	0.30954
3300	0.57030	0.16888	0.22508	0.29935
3600	0.56416	0.16797	0.22167	0.29071
3900	0.55893	0.16719	0.21876	0.28338
4200	0.55451	0.16652	0.21628	0.27720
4500	0.55084	0.16597	0.21422	0.27205
4800	0.54786	0.16552	0.21253	0.26785
5121	0.54544	0.16516	0.21114	0.26440
5400	0.54385	0.16492	0.21023	0.26215
5700	0.54260	0.16473	0.20952	0.26038
6000	0.54182	0.16461	0.20907	0.25927
6300	0.54149	0.16456	0.20888	0.25880
6371	0.54147	0.16455	0.20887	0.25878

Table 5 — Deformation Coefficients for the Equipotential Surfaces, Earth Model 1066A

Depth (km)	$-10^6 \cdot f_0$	$-10^2 \cdot f_2$	$+10^5 \cdot f_4$	$-10^8 \cdot f_6$
0	0.99376	0.22293	0.44762	0.96520
11	0.99175	0.22271	0.44662	0.96181
300	0.94067	0.21690	0.42135	0.87799
421	0.92023	0.21453	0.41137	0.84631
671	0.87929	0.20970	0.39158	0.78609
900	0.84230	0.20524	0.37364	0.73341
1200	0.79357	0.19922	0.34946	0.66318
1500	0.74509	0.19303	0.32462	0.59144
1800	0.69795	0.18683	0.29953	0.51888
2100	0.65390	0.18084	0.27511	0.44758
2400	0.61557	0.17545	0.25295	0.38177
2887	0.57738	0.16992	0.23032	0.31392
3000	0.57402	0.16943	0.22856	0.30950
3300	0.56562	0.16818	0.22422	0.29879
3600	0.55776	0.16701	0.22026	0.28929
3900	0.55019	0.16587	0.21661	0.28088
4200	0.54243	0.16470	0.21302	0.27310
4500	0.53381	0.16339	0.20913	0.26512
4800	0.52371	0.16183	0.20435	0.25515
5142	0.51382	0.16030	0.19902	0.24213
5400	0.51187	0.15999	0.19801	0.23985
5700	0.50964	0.15964	0.19688	0.23738
6000	0.50787	0.15937	0.19600	0.23542
6300	0.50686	0.15921	0.19552	0.23442
6371	0.50674	0.15919	0.19547	0.23430

Table 6 — Deformation Coefficients for the Equipotential Surfaces, Earth Model QM2

Depth (km)	$-10^6 \cdot f_0$	$-10^2 \cdot f_2$	$+10^5 \cdot f_4$	$-10^8 \cdot f_6$
0	0.99239	0.22278	0.44648	0.96148
3	0.99184	0.22272	0.44620	0.96055
21	0.98857	0.22235	0.44457	0.95501
300	0.93931	0.21674	0.42010	0.87363
671	0.87834	0.20959	0.39047	0.78217
900	0.84170	0.20517	0.37269	0.73006
1200	0.79336	0.19919	0.34864	0.66024
1500	0.74531	0.19306	0.32392	0.58877
1800	0.69871	0.18693	0.29903	0.51666
2100	0.65530	0.18103	0.27485	0.44588
2400	0.61776	0.17577	0.25301	0.38077
2886	0.58122	0.17049	0.23104	0.31431
3000	0.57827	0.17005	0.22942	0.31013
3300	0.57118	0.16901	0.22555	0.30029
3600	0.56497	0.16809	0.22222	0.29198
3900	0.55927	0.16724	0.21921	0.28471
4200	0.55385	0.16643	0.21640	0.27801
4500	0.54875	0.16566	0.21377	0.27189
4800	0.54396	0.16493	0.21129	0.26620
5156	0.53932	0.16423	0.20866	0.25960
5400	0.53853	0.16411	0.20807	0.25791
5700	0.53832	0.16407	0.20783	0.25716
6000	0.53770	0.16398	0.20751	0.25642
6300	0.53681	0.16384	0.20707	0.25546
6371	0.53681	0.16384	0.20707	0.25545

Table 7 shows the surface values (i.e., those values for $a = a_1$) of the f's and of the coefficients K appearing in the spherical harmonic expansion of the potential according to the formula

$$V_0(r, \cos\theta, a_1) = \frac{Gm_1}{r}\left[1 + \sum_{j=1}^{\infty} K_{2j}(a_1)\left(\frac{a_1}{r}\right)^{2j} P_{2j}(\cos\theta)\right]. \qquad (16)$$

Also shown is the value of the ellipticity,

$$\epsilon = \frac{r(a_1, 0) - r(a_1, 1)}{r(a_1, 0)}, \qquad (17)$$

and of the ratio $(C - A)/C$, where A is the moment of inertia with respect to any barycentric axis in the equatorial plane and C the moment of inertia with respect to the polar axis. This table is a comparison of four Earth density models and includes the results for the Bullen model, which required only 387 pivotal points for reaching the same accuracy.

Table 7 — Comparison of Earth Density Models*

Parameter	QM2	1066A	HB_1	Bullen (1940)
$f_0\ (a_1)$	$-0.99239 \cdot 10^{-6}$	$-0.99376 \cdot 10^{-6}$	$-0.99421 \cdot 10^{-6}$	$-0.10098 \cdot 10^{-5}$
$f_2\ (a_1)$	$-0.22278 \cdot 10^{-2}$	$-0.22293 \cdot 10^{-2}$	$-0.22298 \cdot 10^{-2}$	$-0.22473 \cdot 10^{-2}$
$f_4\ (a_1)$	$+0.44648 \cdot 10^{-5}$	$+0.44762 \cdot 10^{-5}$	$+0.44766 \cdot 10^{-5}$	$+0.45202 \cdot 10^{-5}$
$f_6\ (a_1)$	$-0.96148 \cdot 10^{-8}$	$-0.96520 \cdot 10^{-8}$	$-0.96569 \cdot 10^{-8}$	$-0.97129 \cdot 10^{-8}$
$K_2\ (a_1)$	$-0.10735 \cdot 10^{-2}$	$-0.10751 \cdot 10^{-2}$	$-0.10756 \cdot 10^{-2}$	$-0.10929 \cdot 10^{-2}$
$K_4\ (a_1)$	$+0.29625 \cdot 10^{-5}$	$+0.29763 \cdot 10^{-5}$	$+0.29776 \cdot 10^{-5}$	$+0.30495 \cdot 10^{-5}$
$K_6\ (a_1)$	$-0.11199 \cdot 10^{-7}$	$-0.11284 \cdot 10^{-7}$	$-0.11293 \cdot 10^{-7}$	$-0.11598 \cdot 10^{-7}$
ϵ^{-1}	299.8	299.6	299.6	297.2
$A = Ie$	$0.80087 \cdot 10^{35}$	$0.80168 \cdot 10^{35}$	$0.80212 \cdot 10^{35}$	$0.80893 \cdot 10^{35}$
$C = Ip$	$0.80347 \cdot 10^{35}$	$0.80429 \cdot 10^{35}$	$0.80473 \cdot 10^{35}$	$0.81159 \cdot 10^{35}$
$(C-A)/C$	$0.3239 \cdot 10^{-2}$	$0.3242 \cdot 10^{-2}$	$0.3243 \cdot 10^{-2}$	$0.3274 \cdot 10^{-2}$

*q = 0.00115

We remark here that the geodetic values obtained from satellite measurements lie between the data for the Bullen and the HB1 models. Such deviations can be assumed to represent a measure of the role the elastic energy plays in the rotational deformation of the Earth.

Notice also the apparent tendency of the three new models to converge toward limiting values of the parameters, a trend that augurs well for the future knowledge of a real Earth model.

DEFORMATIONS OF JUPITER AND SATURN

Jupiter and Saturn comprise about 90% of the total mass of the planetary system; therefore, the great interest which in recent years has arisen toward developing a density model for their interior and ascertaining the oblateness of their exterior shape is quite understandable.

Pioneering work on Jupiter's internal composition goes back to Wildt [10] and Ramsey [11]. Their theory was further elaborated by DeMarcus [12], Opik [13], and Peebles [14]. More recently, Podolak and Cameron [15], Zharkov et al. [16], and Slattery [17] have contributed to the topic.

In the above mentioned works, the Jupiter interior is conceived as a hydrogen and helium envelope approximately in the solar mixture surrounding a core of heavy elements. By solar mixture we mean that the hydrogen mass fraction is 0.78 and the helium mass fraction is 0.22. Within this gaseous envelope, one can distinguish primarily three layers beginning with a very low density region that can be treated adequately with perfect gas laws, a transition region of gas mixture in a molecular state where the Van der Waals equation can be applied, and a metallic hydrogen region for which the equation of state is also known. The various models which have been considered differ primarily because of the equation of state adopted for the transition region.

Saturn's models have evolved concomitantly with Jupiter's. However, since Saturn is smaller than Jupiter, more of the planet's interior is expected to be in the molecular state, and thus more uncertain in its composition.

DeMarcus [12] made use of the second-order theory of hydrostatic equilibrium as developed by DeSitter [18] and recast it into a form which is very suitable for ascertaining the density profile of a planet when only the equation of state is known.

Notwithstanding claims made later by Slattery [17], Zharkov [16] used only a second-order theory in developing Jupiter's density profile. To be more specific, in 1968 Zharkov [19] did develop a third-order equilibrium theory which appeared in English translation in *Soviet Astronomy* (1970); however, he limited himself to obtaining integral relationships basically equivalent to those already achieved by Lanzano in 1962 [20]. The complicated form assumed by Zharkov's equations makes it unlikely that he could have used such theory to obtain Jupiter's density profile.

Slattery [17] developed two Jupiter models in accordance with which core density reached values of 13 and 22 g/cm^3. In developing these models, he used a fourth-order theory elaborated by Hubbard et al. [21]. This theory is objectionable not only from a theoretical point of view because no use is made of the equipotential surfaces, but also from a computational viewpoint because of the doubtful convergence of the expressions therein considered.

Because of these drawbacks, in the present work we use the well-tested DeMarcus density profile (Table 8) in conjunction with the third-order theory of Kopal and Lanzano to obtain more accurate values for the deformation coefficients of the equipotential surfaces and for the coefficients of the harmonics in the exterior potential. This third-order theory is the analytic elaboration of our already mentioned 1962 results, whereby we were successful in transforming, by means of differentiation and elimination operations, a rather intricate system of integral equations into a simple system of second-order ordinary differential equations with boundary conditions.

The initial data we used for Jupiter and Saturn have been taken from Brouwer and Clemence [22] and are summarized in Table 9.

Table 8 — DeMarcus Density Profiles for Major Planets

Jupiter				Saturn			
Depth (km)	ρ (g/cm^3)	Depth	ρ	Depth	ρ	Depth	ρ
0	0.00016	17,465	1.31	0	0.00016	23,052	0.611
140	0.032	20,958	1.56	288	0.023	25,934	0.678
279	0.103	24,451	1.83	576	0.092	27,507	0.719
419	0.138	27,944	2.12	864	0.125	27,507	0.999
559	0.162	31,437	2.40	1,153	0.151	28,815	1.048
699	0.181	34,931	2.66	1,441	0.170	31,697	1.163
741	0.185	38,424	2.90	1,729	0.185	34,578	1.289
741	0.197	41,917	3.14	1,729	0.197	37,460	2.166
1,397	0.246	45,410	3.37	2,882	0.236	40,341	4.16
4,192	0.367	48,903	3.58	4,322	0.268	43,223	6.73
6,986	0.479	52,396	3.81	5,763	0.293	46,104	9.45
9,781	0.593	55,889	4.08	8,645	0.347	48,986	11.93
12,575	0.714	59,382	4.40	11,526	0.397	51,867	13.94
13,832	0.777	62,875	19.09	14,408	0.446	54,749	15.18
13,832	1.08	66,368	27.90	17,289	0.498	57,630	15.62
13,972	1.09	69,861	30.84	20,171	0.552		

Table 9 — Data of Brouwer and Clemence for Major Planets*

Parameter	Jupiter	Saturn
m_1	$1.902 \cdot 10^{30}$g	$0.5694 \cdot 10^{30}$g
a_1	$6.9861 \cdot 10^{9}$cm	$5.763 \cdot 10^{9}$cm
$\bar{\rho}_0\ (a_1)$	1.33 g/cm^3	0.71 g/cm^3
$\rho_0\ (0)$	30.84 g/cm^3	15.62 g/cm^3
T	9.87 hr	10.41 hr
ω	$1.768317 \cdot 10^{-4}$sec^{-1}	$1.676589 \cdot 10^{-4}$sec^{-1}
q	$0.28004 \cdot 10^{-1}$	$0.47207 \cdot 10^{-1}$

*Fundamental parameters used in the integration.

Results of the Pioneer 10 and 11 missions gave rise to revised data for Jupiter (see Anderson et al., [23]), primarily for its radius $a_1 = 7.14 \cdot 10^9$ cm, and its rotational period $T = 9.925$ hours, whereby $q = 0.0296$. We have, however, used the older set of data not only for the sake of comparison with Kopal's results, but also because we do not believe that the newer data would have changed the results appreciably.

Our results are summarized in Table 10. To achieve accurate solutions, we had to take 284 pivotal points in the integration of Jupiter's deformations, and 401 points in the case of Saturn's. The ellipticity, ϵ, is 0.064433 for Jupiter and 0.097847 for Saturn.

We compare our results with the following:

- Observational results of Brouwer and Clemence and of Anderson et al. (Table 11);
- 1963 results by James and Kopal (Table 12), where the DeMarcus profile and a second-order theory were used; and
- results in 1977 by Slattery (Table 13); he used a fourth-order approximation, the new data, and a different density profile.

THE LINEARIZED NAVIER-STOKES EQUATION FOR AN ELASTIC EARTH

To go one step further and consider a realistic model of the Earth, we must take into account the effect of the elastic forces. For this purpose, we assume that the additional stress field τ_{ij} and the corresponding displacement field u_i, measured from the reference state, are related according to the relationship

$$\tau_{ij} = \lambda \frac{\partial u_k}{\partial x_k} \delta_{ij} + \mu \left(\frac{\partial u_i}{\partial x_j} + \frac{\partial u_j}{\partial x_i} \right). \qquad (18)$$

Table 10 — Surface Values for Major Planets

Parameter	Jupiter (q = 0.028004)	Saturn (q = 0.047207)
f_0 (a_1)	$-0.39517 \cdot 10^{-3}$	$-0.94731 \cdot 10^{-3}$
f_2 (a_1)	$-0.44701 \cdot 10^{-1}$	$-0.69585 \cdot 10^{-1}$
f_4 (a_1)	$+0.20037 \cdot 10^{-2}$	$+0.57156 \cdot 10^{-2}$
f_6 (a_1)	$-0.91101 \cdot 10^{-4}$	$-0.42411 \cdot 10^{-3}$
K_2 (a_1)	$-0.15013 \cdot 10^{-1}$	$-0.18465 \cdot 10^{-1}$
K_4 (a_1)	$+0.68165 \cdot 10^{-3}$	$+0.15885 \cdot 10^{-2}$
K_6 (a_1)	$-0.39233 \cdot 10^{-4}$	$-0.15591 \cdot 10^{-3}$
ϵ^{-1}	15.52	10.22
$A = I_e$	$0.23691 \cdot 10^{40}$	$0.39762 \cdot 10^{39}$
$C = I_p$	$0.25068 \cdot 10^{40}$	$0.43157 \cdot 10^{39}$
$(C\text{-}A)/C$	$0.5494 \cdot 10^{-1}$	$0.7867 \cdot 10^{-1}$

Table 11 — Results of Brouwer and Clemence and of Anderson

Parameter	Jupiter		Saturn
	*	**	*
K_2	$-0.147066 \cdot 10^{-1}$	$-0.1472 \cdot 10^{-1}$	$-0.166733 \cdot 10^{-1}$
K_4	$0.674666 \cdot 10^{-3}$	$0.65 \cdot 10^{-3}$	$0.102933 \cdot 10^{-2}$
ϵ	$\frac{1}{15.34} = 0.0651890$		$\frac{1}{10.21} = 0.0979432$

*Brouwer and Clemence (1961)
**Anderson et al. (1974)

Table 12—Data of James and Kopal (1963)

Parameter	Jupiter	Saturn
f_2	$-0.4409 \cdot 10^{-1}$	$-0.6930 \cdot 10^{-1}$
f_4	$0.202 \cdot 10^{-2}$	$0.594 \cdot 10^{-2}$
K_2	$-0.1440 \cdot 10^{-1}$	$-0.1797 \cdot 10^{-1}$
K_4	$0.5667 \cdot 10^{-3}$	$0.1302 \cdot 10^{-2}$
ϵ	$0.0634518 = \frac{1}{15.76}$	$0.0968054 = \frac{1}{10.33}$
$\frac{C-A}{C}$	0.0525	0.0768

The De Marcus profile and second-order theory were used.

Table 13—Data of Slattery (1977)

Parameter	Jupiter	Saturn
K_2	$-0.1478 \cdot 10^{-1}$	$-0.1667 \cdot 10^{-1}$
K_4	$0.605 \cdot 10^{-3}$	$0.0953 \cdot 10^{-2}$
K_6	$-0.37 \cdot 10^{-4}$	$-0.081 \cdot 10^{-3}$
ϵ	0.06527	0.1006

Fourth-order approximation, new data, and a different density profile were used.

This formula, in which use has been made of the summation convention, is valid for a perfectly elastic and isotropic medium. Here λ and μ are the Lamé elastic parameters; μ is also known as the rigidity. These two parameters are related to the incompressibility or bulk modulus by the relationship

$$k = \lambda + \frac{2}{3} \mu . \qquad (19)$$

Within the validity of the infinitesimal deformation theory we can safely assume that equation (18) applies to the coordinates that the points of the medium had before the occurrence of deformation. This assumption cannot, however, be made for the initial stress field; as a consequence, the total stress field at the undeformed points must be written as

$$\sigma_{ij} = T_{ij} - \frac{\partial T_{ij}}{\partial x_k} u_k + \tau_{ij} . \qquad (20)$$

With respect to an inertial frame, the equations representing the deviation from the reference state are

$$\rho \frac{d^2 u_i}{dt^2} = \rho \frac{\partial V}{\partial x_i} + \frac{\partial \sigma_{ij}}{\partial x_j} . \qquad (21)$$

ρ is the mass density and is the sum of two terms:

$$\rho = \rho_0 + \rho_1 ,$$

where ρ_1, the change due to the displacement field u_i is given by the continuity equation

$$\rho_1 = - \frac{\partial}{\partial x_i} (\rho_o u_i) . \qquad (22)$$

$V = V_0 + V_1$ is the total potential, where V_1 satisfies the Poisson equation

$$\nabla^2 V_1 = -4\pi G \rho_1 . \qquad (23)$$

The components of gravity will then appear to be

$$g_i = g_{0,i} + g_{1,i} , \qquad (24)$$

where $g_{1,i} = \frac{\partial V_1}{\partial x_i}$.

Neglecting the product $\rho_1 g_{1,i}$, since it is of the second order in the displacements, and considering that

$$\frac{\partial T_{ij}}{\partial x_k} = - \frac{\partial p_0}{\partial x_k} \delta_{ij} = -\rho_0 g_{0,k} \delta_{ij} ,$$

we arrive at the following:

$$\rho \frac{d^2 u_i}{dt^2} = \rho_0 g_{1,i} + \rho_1 g_{0,i} + \frac{\partial}{\partial x_i} (\rho_0 g_{0,k} u_k) + \frac{\partial \tau_{ij}}{\partial x_j} . \qquad (25)$$

Note that equations (1), (20) and (21) have been used in obtaining it. The last term in equation (25), when expanded, yields

$$\frac{\partial \tau_{ij}}{\partial x_j} = \left(\frac{\partial \lambda}{\partial x_j}\frac{\partial u_k}{\partial x_k} + \lambda \frac{\partial^2 u_k}{\partial x_j \partial x_k}\right)\delta_{ij} + \mu\left(\frac{\partial^2 u_i}{\partial x_j \partial x_j} + \frac{\partial^2 u_j}{\partial x_i \partial x_j}\right) + \frac{\partial \mu}{\partial x_j}\left(\frac{\partial u_i}{\partial x_j} + \frac{\partial u_j}{\partial x_i}\right). \quad (26)$$

The reduction of the previous expressions to vectorial notation can be accomplished by taking into account the following facts:

1) $\frac{\partial u_k}{\partial x_k} = \nabla \cdot \mathbf{u}$ is the dilatation Δ;

2) $\frac{\partial^2 u_k}{\partial x_i \partial x_k} = \frac{\partial^2 u_j}{\partial x_i \partial x_j}$ is the ith component of the gradient of the dilatation, $\nabla(\nabla \cdot \mathbf{u})$;

3) $\frac{\partial^2 u_i}{\partial x_j \partial x_j}$ is the ith component of the vector Laplacian $\nabla^2 \mathbf{u}$, which is known to be representable according to the vector identity $\nabla^2 \mathbf{u} = \nabla(\nabla \cdot \mathbf{u}) - \nabla \times \nabla \times \mathbf{u}$;

4) Finally one can prove (see the Appendix for details) that the expression

$$\frac{\partial \mu}{\partial x_j}\left(\frac{\partial u_i}{\partial x_j} + \frac{\partial u_j}{\partial x_i}\right)$$

is the ith component of the vector

$$(\nabla \mu)(\nabla \cdot \mathbf{u}) + \nabla(\mathbf{u} \cdot \nabla \mu) + \nabla \times (\mathbf{u} \times \nabla \mu) - \mathbf{u}\nabla^2 \mu. \quad (27)$$

Replacing the above vector quantities within equations (25) and (26), one gets

$$\rho \frac{d^2 \mathbf{u}}{dt^2} = \rho_0 \mathbf{g}_1 + \rho_1 \mathbf{g}_0 + \nabla(\rho_0 \mathbf{u} \cdot \mathbf{g}_0) + (\lambda + 2\mu)\nabla(\nabla \cdot \mathbf{u}) \quad (28)$$

$$-\mu \nabla \times \nabla \times \mathbf{u} + (\nabla \lambda + \nabla \mu)(\nabla \cdot \mathbf{u}) + \nabla(\mathbf{u} \cdot \nabla \mu) + \nabla \times (\mathbf{u} \times \nabla \mu) - \mathbf{u}\nabla^2 \mu .$$

This is essentially the Navier-Stokes equation when allowance is made for the variation of the material's elastic parameters and when quadratic terms in the displacements are dropped. λ, μ, and ρ_0 are supposed to be known functions of the radial distance. As a matter of fact, it easily follows from equations (13) and (19) that the Lame parameters are related to the *P* and *S* seismic velocities according to

$$\rho_0 \alpha^2 = \lambda + 2\mu; \quad \rho_0 \beta^2 = \mu.$$

Consequently, their expressions as functions of the radial distance or depth can be obtained from the density and the velocity of seismic waves. Their values are provided by the Earth model tables.

$\mathbf{g}_0$ and $\mathbf{g}_1$ are obtainable from V_0 and V_1, respectively, via the Poisson equations (4) and (23); on the other hand, ρ_1 is obtainable from the continuity equation (22).

The acceleration of **u** with respect to an inertial frame is given by

$$\frac{d^2\mathbf{u}}{dt^2} = \frac{\partial^2\mathbf{u}}{\partial t^2} + 2\omega \times \frac{\partial \mathbf{u}}{\partial t} + \frac{d\omega}{dt} \times \mathbf{u} + (\omega \cdot \mathbf{u})\,\omega - \omega^2\mathbf{u}, \qquad (29)$$

where the symbol of partial derivative refers to the variation of a vector with respect to the rotating frame. If we want to ascertain a permanent deformation, the vector **u**, measured with respect to a rotating Earth, should be independent of time; this means that

$$\frac{\partial^2\mathbf{u}}{\partial t^2} = \frac{\partial \mathbf{u}}{\partial t} = 0.$$

Also, in the case of a constant angular rate and of no variation in the position of the rotational axis, one should have

$$\frac{d\omega}{dt} = 0.$$

Therefore, we are left with the expression

$$\frac{d^2\mathbf{u}}{dt^2} = (\omega \cdot \mathbf{u})\,\omega - \omega^2\mathbf{u}. \qquad (30)$$

Using equation (30), we find that the left-hand side of equation (28) becomes

$$\rho_0 \left[(\omega \cdot \mathbf{u})\,\omega - \omega^2\mathbf{u}\right], \qquad (31)$$

where the term $\rho_1\mathbf{u}$ has been neglected because it is of the second order in the displacements.

When the left-hand side is replaced by equation (31), equation (28) represents the fundamental relation which yields the perturbation displacement **u**. One should seek solutions to this equation in the form of spheroidal and toroidal deformations as expressed by equation (14).

DISCUSSION OF THE RESULTS

We have developed a general equilibrium theory which has two functions:

(1) It yields the fundamental state of deformation for a rotating body in the presence of hydrostatic forces; this can be accomplished by solving the Clairaut equation with boundary conditions; and

(2) It accounts for the additional deformations attributable to elastic forces as perturbations to the previously obtained fundamental mode; the perturbation equation in question is a linearized version of the Navier-Stokes equation.

For the Earth we have numerically solved the Clairaut equation using various density profiles and have compared our results with well established satellite-obtained data pertaining to the second, fourth, and sixth harmonics of the geopotential. The observed discrepancies are primarily due to the presence of shear stresses and convection currents in the Earth's mantle. To remedy this situation, one must solve the Navier-Stokes perturbation equation; this we plan to do in the near future as our next task.

In the case of the two giant planets, our results represent an improvement on Kopal's previous work, which was based on the second-order Clairaut equation and the same DeMarcus density model. Our results compare favorably with recent work by Hubbard and Slattery, who use a different density distribution, primarily because of our more advanced mathematical formulation: preliminary analytical work has allowed us to simplify the original equilibrium conditions which as used by those authors were expressed by a complicated integro-differential relationship; we obtained a well-posed boundary value problem consisting of the Clairaut equation. This feature of simplicity is responsible for obtaining more accurate solutions more rapidly.

A preliminary version of these results was presented orally at the Spring Meeting of the American Geophysical Union in Miami Beach, April 1978.

ACKNOWLEDGMENTS

The authors wish to thank Mrs. Dolores Fortin for her work beyond the call of duty in typing the original version of the manuscript.

Appendix

MATHEMATICAL PROOF OF A VECTOR IDENTITY

From the definitions

$$(\mathbf{u} \times \nabla\mu)_n = \epsilon_{njk}\, u_j \frac{\partial \mu}{\partial x_k} \qquad \text{and}$$

$$(\nabla \times \mathbf{u})_i = \epsilon_{imn} \frac{\partial u_n}{\partial x_m},$$

where ϵ is the completely antisymmetric third-rank tensor (also known as the permutation symbol or Levi-Civita density), one gets the following:

$$[\nabla \times (\mathbf{u} \times \nabla\mu)]_i = \epsilon_{imn} \frac{\partial}{\partial x_m} \left(\epsilon_{njk} u_j \frac{\partial \mu}{\partial x_k} \right)$$

$$= \epsilon_{imn}\epsilon_{njk} \left(\frac{\partial u_j}{\partial x_m} \frac{\partial \mu}{\partial x_k} + u_j \frac{\partial^2 \mu}{\partial x_k \partial x_m} \right)$$

$$= \frac{\partial u_i}{\partial x_k} \frac{\partial \mu}{\partial x_k} - \frac{\partial u_j}{\partial x_j} \frac{\partial \mu}{\partial x_i} + u_i \frac{\partial^2 \mu}{\partial x_k \partial x_k} - u_j \frac{\partial^2 \mu}{\partial x_i \partial x_j}. \qquad (1\text{A})$$

Here use has been made of the property that ϵ is antisymmetric for an interchange of any pair of indices, whereby

$$\epsilon_{njk} = \epsilon_{jkn}\,;$$

also the tensor identity,

$$\epsilon_{imn}\epsilon_{jkn} = \delta_{ij}\delta_{mk} - \delta_{ik}\delta_{mj},$$

was used — see, e.g., Harris [24] pp. 10-13.

Using equation (1A), one can express the *i*th component of the vector represented by equation (27) as

$$\frac{\partial \mu}{\partial x_i}\frac{\partial u_k}{\partial x_k} + \frac{\partial}{\partial x_i}\left(u_k \frac{\partial \mu}{\partial x_k}\right) - u_i \frac{\partial^2 \mu}{\partial x_j \partial x_j} + \frac{\partial u_i}{\partial x_k}\frac{\partial \mu}{\partial x_k}$$

$$- \frac{\partial u_j}{\partial x_j}\frac{\partial \mu}{\partial x_i} + u_i \frac{\partial^2 \mu}{\partial x_k \partial x_k} - u_j \frac{\partial^2 \mu}{\partial x_i \partial x_j} = \frac{\partial \mu}{\partial x_k}\left(\frac{\partial u_i}{\partial x_k} + \frac{\partial u_k}{\partial x_i}\right). \qquad \text{q.e.d.}$$

REFERENCES

1. P. Lanzano, *Astrophys. Space Science*, 29, 161 (1974).

2. Z. Kopal and P. Lanzano, "Third-Order Clairaut Equation for a Rotating Body of Arbitrary Density and Its Application to Marine Geodesy," NRL Report 7801 (1974).

3. P. Lanzano and J. C. Daley, *AIAA Journal*, 15, 1231 (1977).

4. R. James and Z. Kopal, *Icarus*, 1, 442 (1963).

5. K. E. Bullen, "An Introduction to the Theory of Seismology," Third Revised Edition, Cambridge Univ. Press, pp. 227-240 (1963).

6. R. A. W. Haddon and K. E. Bullen, *Phys. Earth Planet. Interiors*, 2, 35 (1969).

7. R. S. Hart, D. L. Anderson, and H. Kanamori, *J. Geophys. Res.*, 82, 1647 (1977).

8. F. Gilbert and A. M. Dziewonski, *Phil. Trans. Roy. Soc.*, London (A) 278, 187 (1975).

9. L. Fox, "The Numerical Solution of Two-Point Boundary Problems in Ordinary Differential Equations," Oxford Univ. Clarendon Press, pp. 67-68 and 328-332 (1957).

10. R. Wildt, *Month. Not. Roy. Astron. Soc.*, 107, 82 (1947).

11. W. H. Ramsey, *Month. Not. Roy. Astron. Soc.*, 111, 427 (1951).

12. W. C. DeMarcus, *Astron. J.*, 63, 2 (1958).

13. E. J. Öpik *Icarus*, 1, 200 (1962).

14. P. J. E. Peebles, *Astrophys. J.*, 140, 328 (1964).

15. M. Podolak and A. G. W. Cameron, *Icarus*, 22, 123 (1974).

16. V. N. Zharkov, A. B. Makalkin, and V. P. Trubitsyn, *Sov. Astron.*, 18, 768 (1975).

17. W. L. Slattery, *Icarus*, 32, 58 (1977).

18. W. DeSitter, *Bull. Astron. Inst. Neth.*, 2, 97 (1924).

19. V. N. Zharkov and V. P. Trubitsyn, *Sov. Astron*,. 13, 981 (1970).

20. P. Lanzano, *Icarus*, 1, 121 (1962).

21. W. B. Hubbard, W. L. Slattery, and C. L. DeVito, *Astrophys. J.*, 199, 504 (1975).

22. D. Brouwer and G. M. Clemence, "Orbits and Masses of Planets and Satellites" in *The Solar System* (G. P. Kuiper and B. M. Middlehurst, eds.), Vol. 3, pp. 72-73 Univ. of Chicago Press (1961).

23. J. D. Anderson, G. W. Null, and S.K. Wong, *J. Geophys. Res.* 79, 3661 (1974).

24. E. G. Harris, "Introduction to Modern Theoretical Physics," Vol. 1, J. Wiley, pp. 10-13 (1975).